Coherent vs. Non-Coherent Joint Transmission in Cell-Free User-Centric Non-Terrestrial Wireless Networks

Carmen D'Andrea[1,4], Tommaso Foggi[2,4], Amina Piemonese[2,4], Alessandro Ugolini[2,4], Stefano Buzzi[1,3,4], Giulio Colavolpe [2,4]

[1]*DIEI, University of Cassino and Southern Lazio, 03043 Cassino (FR) – Italy*

[2]*DIA, University of Parma, 43124 Parma (PR) – Italy*

[3]*DEIB, Politecnico di Milano, 20122 Milano (MI) – Italy*

[4]*Consorzio Nazionale Interuniversitario per le Telecomunicazioni, 43124 Parma (PR) – Italy*

E-mail: {carmen.dandrea, buzzi}@unicas.it,{tommaso.foggi, amina.piemontese, alessandro.ugolini, giulio.colavolpe}@unipr.it

***Abstract*—In terrestrial wireless networks, using multiple access points for joint coherent transmission towards mobile users is well known to provide several benefits. Conversely, for non-terrestrial networks (NTNs), the advantages of joint coherent processing are hardly achievable due to the difficulty to achieve perfect phase synchronization among the transmitting devices. This paper thus investigates the limits and challenges related to joint transmission in a cell-free user-centric massive MIMO NTN scenario. In particular, after introducing the transceiver signal processing for satellite-based joint transmission, we analyze through extensive numerical results how the coherent and non-coherent joint transmissions influence the system performance and envisage the need for approaches that achieve an, at least coarse, phase synchronization among transmitting devices to partly restore the system performance.**

***Index Terms*—user-centric, non-terrestrial networks, coherent, non-coherent**

I. Introduction

ONE of the main challenges of future 6G wireless networks is to provide broadband coverage in emergency conditions, such as natural disasters, to avoid connectivity outages. To address these issues, which nowadays are unfortunately far from rare, 6G research is currently focusing on the development of non-terrestrial networks (NTN) to promote ubiquitous and efficient global connectivity [1], [2]. NTN integrate non-terrestrial devices, including UAVs, high-altitude platforms, and space-borne satellites. Among these, low-Earth-orbit (LEO) satellite mega-constellations have attracted a huge interest, both in academia and industry [3].

In LEO mega-constellation scenarios, a line-of-sight (LOS) link between the satellite and the terrestrial user terminal (UT) is not always granted: due to the fast movement of the satellite, the LOS link can be indeed unexpectedly shadowed/obstructed by physical objects nearby the UT. Satellite macro-diversity schemes, i.e., the joint use of several satellites to serve the same UT, can be widely used in order to increase the system reliability and efficiency [4], [5].

This approach requires that the satellites serving the same UT have independent trajectories and are located in different portions of the sky, the individual UT-satellite links may be reasonably assumed to be subject to independent shadowing realizations, thus implying that the overall outage probability decreases exponentially with the number of employed satellites and that the coverage is more uniform. For the above reasons, the practical implementation of satellite diversity poses a number of technical challenges, due to the need to combine at the UT two or more paths possibly arriving at different epochs, and with different Doppler shifts and phases.

The technology that nowadays strongly focuses on macro-diversity in terrestrial networks is doubtless cell-free user-centric massive MIMO (CF-UC), which uses several simple access points (APs) connected to central processing units (CPUs) serving multiple UTs [6], [7]. Indeed, there is a strong similarity between a satellite mega-constellation, made of a huge number of relatively simple satellites connected to terrestrial gateways, and a terrestrial CF-UC deployment with the difference that in a terrestrial CF-UC system, the short distance between the UT and the serving APs makes the system realization less challenging with respect to a non-terrestrial scenario [8]. In NTN with LEO satellites, uplink channel estimation is hardly feasible. Also, phase compensation (usually done in terrestrial CF-UC systems) is difficult to

This work was supported by the European Union under the Italian National Recovery and Resilience Plan (NRRP) of NextGenerationEU, partially from the partnership on "Telecommunications of the Future" (PE00000001 - program "RESTART", Structural Project ITA NTN, Cascade Call INFINITE and Structural Project 6GWINET, Cascade Call SPARKS) and partially from the PRIN 2022 project no. 2022BEXMXN_01 entitled "INSPIRE: Integrated Terrestrial/Space wireless networks for broadband connectivity and IoT services" funded by the Italian Ministry of Universities and Research (MUR). The work of A. Ugolini has also been funded by University of Parma through the action Bando di Ateneo 2022 per la ricerca co-funded by MUR-Italian Ministry of Universities and Research - D.M. 737/2021 - PNR - PNRR - NextGenerationEU. This work has been also funded by the European Union Smart Networks and Services Joint Undertaking Project 5G-STARDUST under Grant Agreement 101096573. The views expressed are those of the authors and do not necessarily represent the project. The Commission is not liable for any use that may be made of any of the information contained therein.

implement. In contrast, timing and Doppler shift compensation for a specific location on the ground can be instead quite easily obtained. The UTs will thus receive one or more signals with different phases and, only for certain positions, the same delay/Doppler shift. Mimicking a CF-UC system for a satellite-based network is thus not a straightforward generalization of the terrestrial deployment, and proper approaches must be designed to achieve the gains theoretically granted by the use of macro-diversity.

This paper investigates the limits and challenges in the joint transmission in CF-UC NTN. Specifically, this work deals with the design and assessment of a multi-satellite diversity scenario using the orthogonal frequency division multiplexing (OFDM) modulation starting from the definition of the system and signal model. Then, we discuss coherent and non-coherent joint transmission schemes and investigate the challenges and limitations. Results highlight the benefits provided by satellite diversity in the case of coherent joint transmission also in presence of some phase uncertainty and provide a discussion to afford the (more realistic) non-coherent joint transmission in the considered scenario. The paper is organized as follows. Section II contains the channel and signal model. Section III is devoted to the description of the joint transmission schemes and of the performance measures, while in Section IV we report and comment the obtained numerical results. Finally, concluding remarks are given in Section V.

II. System Model

We denote by M the number of subcarriers, i.e., $W = \Delta_f M$ is the system bandwidth, with Δ_f the subcarrier spacing and by N number of OFDM symbols, i.e., $T_{frame} = NT$ is the frame duration, with T the symbol duration and $\Delta_f T = 1$. We assume Q single antenna UTs and P satellites equipped with uniform planar arrays (UPAs) with N_S antennas.[1]

A. Channel model

The downlink time-varying channel between the q-th UT and the p-th satellite is the following vector-valued $(1 \times N_S)$-dimensional function:

$$\mathbf{h}_{p,q}(t,\tau) = \rho_{p,q}\mathbf{a}_S(\phi_{p,q},\theta_{p,q})\delta(\tau-\tau_{p,q})e^{j2\pi\nu_{p,q}t}\,, \quad (1)$$

where $\rho_{p,q}$ is the complex gain associated to the path between the q-th UT and the p-th satellite containing the path-loss, shadowing, and clutter loss, $\phi_{p,q}$ and $\theta_{p,q}$ are the azimuth and elevation angles of departure (AoD), $\tau_{p,q}$ and $\nu_{p,q}$ are the residual propagation delay and the Doppler shift, $\mathbf{a}_S(\varphi,\vartheta)$ is the uniform planar array (UPA) array response at the satellite. We assume that the satellites perfectly compensate for delay and Doppler shifts at one point on the Earth for each user, that we call *ideal UT position*. Then, we denote an *offset distance* of the UT from the ideal position, $r_{p,q}$ say, which entails residual uncompensated delay and Doppler shifts, i.e. $\tau_{p,q}$ and $\nu_{p,q}$ [4], [5].

[1]In this paper, all satellites have the same number of antennas for the sake of simplicity, but this assumption can be easily removed using a more general notation.

Upon defining the wave vector $\mathbf{k}(\varphi,\vartheta)$ as

$$\mathbf{k}(\varphi,\vartheta) = \frac{2\pi}{\lambda}\left[\cos\vartheta\cos\varphi, \cos\vartheta\sin\varphi, \sin\vartheta\right]^T, \quad (2)$$

with λ the signal carrier wavelength, the array response is written as

$$\mathbf{a}_S^T(\varphi,\vartheta) = \sqrt{\Gamma}\left[e^{j\mathbf{k}^T(\varphi,\vartheta)\mathbf{u}_S(1)}, \ldots, e^{j\mathbf{k}^T(\varphi,\vartheta)\mathbf{u}_S(N_S)}\right], \quad (3)$$

where $N_S = N_{S,X}N_{S,Y}$ is the number of antennas at the satellite with $N_{S,X}$ and $N_{S,Y}$ the number of antennas on the vertical and horizontal axis, respectively, $\mathbf{u}_S(n),\ \forall n$ is the position of the n-th antenna on the satellite and Γ is the gain of the generic radiation element at the satellite [9].

B. Signal model

We focus on a generic block of NM symbols, belonging to a QAM constellation, and denote by $x_{k,\ell}^{(q)}$ the symbol intended to the q-th UT on the downlink in the delay-Doppler domain, with $k = 0,\ldots,N-1$ and $\ell = 0,\ldots,M-1$. We denote by $\alpha_{p,q}$ a binary variable being 1 if the p-th satellite serves the q-th UT and 0 otherwise and by $\mathbf{w}^{(p,q)}$ the N_S-dimensional beamforming vector used at the p-th satellite to serve the q-th UT. Assuming some uncertainty on the knowledge of the UTs' position at the satellites, we denote by $\overline{\phi}_{p,q}, \overline{\theta}_{p,q}$, the *approximate position* of the q-th UT known by the p-th satellite. In this paper, we consider a beamforming technique in which the p-th satellite uses a beam aligned to the approximate position of the q-th UT, i.e.,

$$\mathbf{w}^{(p,q)} = \frac{\mathbf{a}_S^*\left(\overline{\phi}_{p,q},\overline{\theta}_{p,q}\right)}{\left\|\mathbf{a}_S\left(\overline{\phi}_{p,q},\overline{\theta}_{p,q}\right)\right\|}. \quad (4)$$

Considering a standard OFDM modulation with cyclic prefix (CP) in order to avoid the inter-symbol interference (ISI), the resulting OFDM symbol duration is $T_0 = T_{\mathrm{CP}} + T$, where T_{CP} and T denote the duration of CP and data symbols, respectively.

The continuous-time OFDM transmitted signal with CP at the p-th satellite is the following N_S-dimensional continuous time function

$$\mathbf{s}_p(t) = \sum_{q=0}^{Q-1}\alpha_{p,q}\sqrt{\eta_{p,q}}\mathbf{w}^{(p,q)}\sum_{n=0}^{N-1}\sum_{m=0}^{M-1}\widetilde{x}_{n,m}^{(p,q)} \mathrm{rect}(t-nT)e^{j2\pi m\Delta_f(t-nT_0-T_{\mathrm{CP}})}, \quad (5)$$

where $\widetilde{x}_{n,m}^{(p,q)} = x_{n,m}^{(q)}e^{j\delta_{n,m}^{(p,q)}}$, with $\delta_{n,m}^{(p,q)}$ a phase pre-compensation factor that will be discussed in Section III-B. Using the expression of $\mathbf{h}_{p,q}(t,\tau)$ in Eq. (1), the signal received at the q-th UT can be written as

$$r_q(t) = \sum_{p=0}^{P-1}\rho_{p,q}\mathbf{a}_S^T(\phi_{p,q},\theta_{p,q})\mathbf{s}_p(t-\tau_{p,q})e^{j2\pi\nu_{p,q}t} + z_q(t), \quad (6)$$

where $z_q(t)$ denotes the additive white Gaussian noise.

By sampling every T/M and removing the CP in each OFDM symbol, we obtain the signal $r_{n,m}^{(q)}$ which is finally FFTed as

$$y_{n,m}^{(q)} = \frac{1}{M}\sum_{i=0}^{M-1} r_{n,i}^{(q)} e^{-j2\pi\frac{mi}{M}} \tag{7}$$

Using similar computation as in reference [10], and by stacking the received symbols $y_{n,m}^{(q)},\ \forall n,m$ in the NM-dimensional vector $\mathbf{y}^{(q)}$ and the information symbols $x_{n,m}^{(q)},\ \forall n,m$ in the NM-dimensional vector $\mathbf{x}^{(q)}$, we can write the whole observable at the q-th UT as

$$\begin{aligned}\mathbf{y}^{(q)} = &\sum_{p=0}^{P-1} \alpha_{p,q}\sqrt{\eta^{(p,q)}}\overline{\mathbf{\Psi}}^{(p,q,q)}\mathbf{\Delta}^{(p,q)}\mathbf{x}^{(q)} + \\ &\sum_{p=0}^{P-1}\sum_{\substack{q'=0\\q'\neq q}}^{Q-1} \alpha_{p,q'}\sqrt{\eta^{(p,q')}}\overline{\mathbf{\Psi}}^{(p,q,q')}\mathbf{\Delta}^{(p,q')}\mathbf{x}^{(q')} + \mathbf{z}^{(q)},\end{aligned} \tag{8}$$

where

$$\mathbf{\Delta}^{(p,q)} = \text{diag}\left(e^{j\delta_{1,1}^{(p,q)}},\ldots,e^{j\delta_{1,M}^{(p,q)}},\ldots,e^{j\delta_{N,1}^{(p,q)}},\ldots,e^{j\delta_{N,M}^{(p,q)}}\right),$$

and

$$\overline{\mathbf{\Psi}}^{(p,q,q')} = \text{blkdiag}\left(\widetilde{\mathbf{\Psi}}_1^{(p,q,q')},\ldots,\widetilde{\mathbf{\Psi}}_N^{(p,q,q')}\right), \tag{9}$$

with the (m,m')-th entry of the M-dimensional matrix $\widetilde{\mathbf{\Psi}}_n^{(p,q,q')}$ given by

$$\begin{aligned}&\widetilde{\mathbf{\Psi}}_n^{(p,q,q')}(m,m') = \frac{1}{M}\rho_{p,q}\mathbf{a}_S^T(\phi_{p,q},\theta_{p,q}) \\ &\mathbf{w}^{(p,q)}e^{j2\pi nT_0\nu_{p,q}}e^{-j2\pi m'\Delta_f\tau_{p,q}} \\ &\sum_{i=0}^{M-1} e^{j2\pi\frac{i}{M}\frac{\nu_{p,q}}{\Delta_f}}e^{j2\pi\frac{i}{M}(m'-m)}.\end{aligned} \tag{10}$$

III. Joint Transmission and Performance Measures

In this section, we discuss the design of the considered joint transmission schemes and the performance measures used in the numerical results.

A. UT-satellite association and power allocation

For the definition of the binary association variables $\alpha_{p,q}$, we consider the CF-UC approach [6]. Specifically, the q-th UT is served by the N_{UC} satellites that it receives with best average channel conditions. Let $O_q : \{1,\ldots,P\} \to \{1,\ldots,P\}$ denote the sorting operator for the vector $[|\rho_{q,1}|,\ldots,|\rho_{q,P}|]$, such that $|\rho_{q,O_q(1)}| \geq |\rho_{q,O_q(2)}| \geq \ldots \geq |\rho_{q,O_q(P)}|$. Thus, the binary association variables are defined as follows:

$$\begin{cases} \alpha_{O_q(1),q} = \ldots = \alpha_{O_q(N_{\text{UC}}),q} = 1, \\ \alpha_{O_q(N_{\text{UC}}+1),q} = \ldots = \alpha_{O_q(P),q} = 0 \end{cases}. \tag{11}$$

Regarding the transmit power, we assume *uniform power allocation* from each satellite to the UTs that it serves. Denoting by $P_{p,\text{SAT}}$ the total power available at the p-th satellite, the coefficients $\eta^{(p,q)}$ are expressed as:

$$\eta^{(p,q)} = \frac{\alpha_{p,q}P_{p,\text{SAT}}}{MN\sum_{q=1}^{Q}\alpha_{p,q}} \tag{12}$$

B. Coherent and non-coherent joint transmission schemes

We now detail the three possible choices here considered for the phase pre-compensation factor used at the satellites, i.e., $\delta_{n,m}^{(p,q)}$,

i) *perfect coherent joint transmission (PCJT)* where $\delta_{n,m}^{(p,q)} = -\psi_{n,m}^{(p,q)}$, i.e., perfect compensation of the channel phase at the satellites;
ii) *imperfect coherent joint transmission (ICJT)* where $\delta_{p,q} = -\psi_{n,m}^{(p,q)} + u_{p,q}$, with $u_{p,q} \sim \mathcal{U}[-\beta,\beta]$ an uniformly distributed random variate modeling the channel phase uncertainty which does not depend on the symbol, i.e., imperfect compensation of the channel phase at the satellites;
iii) *non-coherent joint transmission (NCJT)* where $\delta_{n,m}^{(p,q)} = 0$, i.e., no compensation of the channel phase at the satellites;

with $\psi_{n,m}^{(p,q)} = \angle\overline{\mathbf{\Psi}}^{(p,q,q)}[(m-1)N+n,(m-1)N+n]$.

C. Performance Measures

The whole observable at the q-th UT can be expressed as in Eq. (8) where the $NM\times NM$-dimensional matrix $\overline{\mathbf{\Psi}}^{(p,q,q')}$ depends on the channel parameters, i.e., $\rho_{p,q},\phi_{p,q},\theta_{p,q},\tau_{p,q},\nu_{p,q}$ and the beamformers $\mathbf{w}^{(p,q')}$. In Section IV, we assess the performance of the considered systems in terms of *signal-to-interference-plus-noise ratio (SINR)* and *pragmatic capacity*. In order to first obtain the expression of the SINR per user and symbol, we assume a "practical" minimum-mean-squares error (MMSE) detection, i.e., $\widehat{\mathbf{x}}^{(q)} = \mathbf{D}_q^H\mathbf{y}^{(q)}$, where we assume at the q-th UT the knowledge of the channels from the serving satellites, i.e.: $\mathbf{D}_q = [\mathbf{A}_q\mathbf{A}_q^H + \sigma_z^2\mathbf{I}_{NM}]^{-1}\mathbf{A}_q$, where $\mathbf{A}_q = \sum_{p=0}^{P-1}\alpha_{p,q}\sqrt{\eta^{(p,q)}}\overline{\mathbf{\Psi}}^{(p,q,q)}\mathbf{\Delta}^{(p,q)}$.

Define $\ell = (m-1)N+n$, the expression of the generic ℓ-th symbol estimated at the q-th UT can be expressed as

$$\begin{aligned}\widehat{\mathbf{x}}^{(q)}(\ell) = &\ \mathbf{D}_q(\ell,:)^H\mathbf{A}_q\mathbf{x}^{(q)} + \mathbf{D}_q(\ell,:)^H\sum_{\substack{q'=0\\q'\neq q}}^{Q-1}\mathbf{A}_q\mathbf{x}^{(q')} + \\ &\mathbf{D}_q(\ell,:)^H\mathbf{z}^{(q)}\end{aligned} \tag{13}$$

Define $i = (n'-1)M+m'$, by exploiting

$$\overline{\mathbf{\Psi}}^{(p,q,q)}\mathbf{\Delta}^{(p,q)}\mathbf{x}^{(q)} = \sum_{i=1}^{NM}\overline{\mathbf{\Psi}}^{(p,q,q)}(:,i)\mathbf{x}^{(q)}(i)e^{j\delta_{n',m'}^{(p,q)}}, \tag{14}$$

and by using the definition of $\mathbf{A}_q$, the expression of the SINR per user and symbol in Eq. (15) at the top of next page is obtained by averaging on symbols and noise realizations.

As already mentioned, the results of this paper are also numerically computed in terms of *pragmatic capacity* [10], i.e., the mutual information of the virtual channel with constellation symbols as input (uniformly distributed) and received samples after the LMMSE processing as soft-outputs, basically providing the achievable rate for separated detection and decoding. Thus, given inputs $\mathbf{x}^{(q)}$ and outputs $\widehat{\mathbf{x}}^{(q)}$, the constellation $\mathcal{C}$ and the set of transmitted symbols, excluding

$$\gamma^{(q)}(\ell)=\frac{\left|\sum_{p=0}^{P-1}\alpha_{p,q}\sqrt{\eta^{(p,q)}}\mathbf{D}_q^H(\ell,:)\overline{\mathbf{\Psi}}^{(p,q,q)}(:,\ell)e^{j\delta_{n,m}^{(p,q)}}\right|^2}{\sum_{\substack{i=1\\ i\neq\ell}}^{NM}\left|\sum_{p=0}^{P-1}\alpha_{p,q}\sqrt{\eta^{(p,q)}}\mathbf{D}_q^H(\ell,:)\overline{\mathbf{\Psi}}^{(p,q,q)}(:,i)e^{j\delta_{n',m'}^{(p,q)}}\right|^2+\sum_{\substack{q'=0\\ q'\neq q}}^{Q-1}\left\|\sum_{p=0}^{P-1}\alpha_{p,q'}\sqrt{\eta^{(p,q')}}\mathbf{D}_q^H(\ell,:)\overline{\mathbf{\Psi}}^{(p,q,q')}\mathbf{\Delta}^{(p,q')}\right\|^2+\sigma_z^2\left\|\mathbf{D}_q(\ell,:)\right\|^2} \tag{15}$$

the pilots, $\mathcal{D}$ (i.e., $|\mathcal{D}|\leq NM$), the pragmatic capacity for q-th UT can be derived as

$$I_{\text{PC}}=\log_2|\mathcal{C}|-\frac{1}{NM}\sum_{k\in\mathcal{D}}P(x_k,\widehat{x}_k)\log_2\frac{1}{P(x_k|\widehat{x}_k)} \tag{16}$$

where $P(x_k|\widehat{x}_k)$ is the *a-posteriori* probability of symbols x_k given the detector soft-outputs $\widehat{x}_k$, whereas $P(x_k,\widehat{x}_k)$ is the joint probability function.

IV. Numerical Results

A. Simulation setup

In the simulated scenario the carrier frequency is $f=5$ GHz (C-band), the subcarrier spacing is $\Delta f=15$ kHz, the symbol time is $T=64$ μs, $M=32$ and $N=50$. The power spectral density of the noise is $N_0=-174$ dBm/Hz and the noise figure at the receiver is $F=5$ dB. We assume $N_{S,X}=N_{S,Y}=8$, i.e., $N_S=64$, $\Gamma=23$ dB, the offset distance $r_{p,q}=1$ km $\forall\, p,q$, and $P_{p,\text{SAT}}=P_{\text{SAT}}=15$ dBW, $\forall\, p=1,\ldots,P$

The considered satellite scenario is based on the Space-X Starlink satellite constellation which is nowadays the closer to be operational, having already more than one thousand satellites in orbit (1584 at the end of the first phase). The final deployment envisages 4408 satellites among 5 shells at 540, 550, 560, 560 and 570 km, respectively. The first shell is the currently in phase of completion (first phase), and, again, the aim is at covering the most populated regions. Table I provides information on the orbital planes.

TABLE I
STARLINK CONSTELLATION ORBITAL PLANES

Altitude (km)	540	550	560	560	570
Inclination (°)	53.2	53	97.6	97.6	70
Number of planes	72	72	6	4	36
Number satellites/plane	22	22	58	43	20

Given the described satellite scenario, the large-scale propagation channel is modeled following the 3GPP TR 38.811 [11], including a log-normal shadowing loss and and a clutter loss (CL), i.e. the attenuation due to surrounding objects on the ground, for non-line-of-sight (NLOS) conditions, where the UT is considered in LOS or NLOS with a probability depending on the elevation angle and type of scenario (rural, urban, sub-urban, dense-urban, table 6.6.1-1 of [11]). In the following results we thus adopt this model by considering the actual elevation angle and a dense-urban scenario (table 6.6.2-1 of [11]), and the corresponding values are reported in Table II.

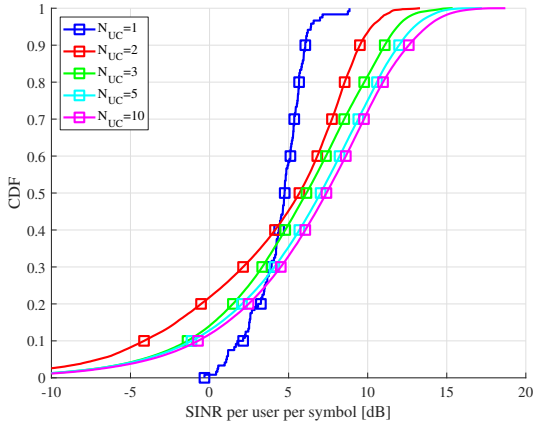

Fig. 1. CDF of the SINR per user and symbol in the case of NCJT for different values of N_{UC}.

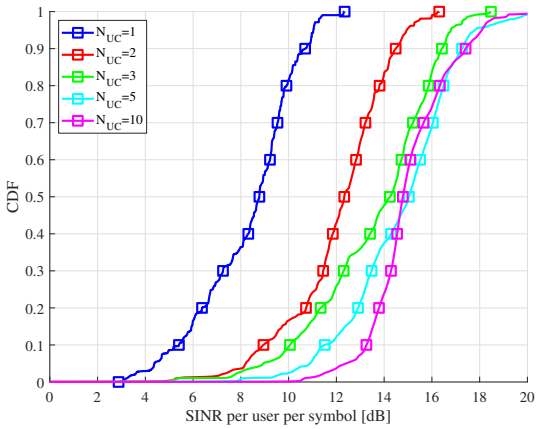

Fig. 2. CDF of the SINR per user and symbol in the case of PCJT for different values of N_{UC}.

B. Performance assessment

In Figs. 1 and 2, we present the performance in terms of SINR per user and per symbol, calculated using Eq. (15), for NCJT and PCJT, respectively. Specifically, Fig. 1 highlights that in the absence of channel phase information, the efficacy of joint transmission is compromised in terms of fairness between users, shown in the lower-left part of the figure, as

TABLE II
3GPP TS 38.811 CHANNEL PARAMETERS FOR DENSE URBAN SCENARIO

Elevation (°)	10	20	30	40	50	60	70	80	90
Probability	28.2%	33.1%	39.8%	46.8%	53.7%	61.2%	73.8%	82.0%	98.1%
LOS σ_{SF} (dB)	3.5	3.4	2.9	3	3.1	2.7	2.5	2.3	1.2
NLOS σ_{SF} (dB)	15.5	13.9	12.4	11.7	10.6	10.5	10.1	9.2	9.2
CL (dB)	34.3	30.9	29.0	27.7	26.8	26.2	25.8	25.5	25.5

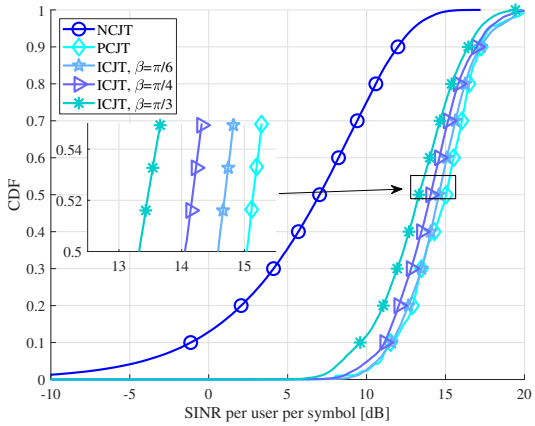

Fig. 3. CDF of the SINR per user and symbol in the cases of NCJT, PCJT and ICJT for different values of β and $N_{\mathrm{UC}} = 5$.

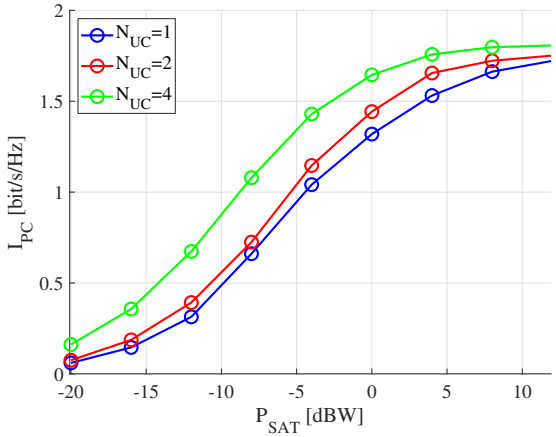

Fig. 4. Pragmatic capacity in the PCJT case for different values of N_{UC}.

evidenced by the superior performance of the state-of-the art solution ($N_{\mathrm{UC}} = 1$). Fig 2 reveals that having knowledge of the channel phase significantly enhances performance and facilitates the constructive combination of multiple signals received at the UT. To assess the system's sensitivity to phase uncertainty, we compare the performance of ICJT for different values of β, i.e., the maximum absolute value for the channel phase uncertainty, in Fig. 3. Remarkably, we observe a high level of robustness in the system against phase uncertainty. Consequently, estimation techniques aimed at providing rough estimates of channel phase can be deemed effective in significantly enhancing performance and leveraging the potential benefits of multi-satellite diversity. Finally, in Fig. 4 we report results in terms of pragmatic capacity, with $N_{\mathrm{UC}} = 1, 2, 4$ in the PCJT case, as a function of the total available power for each satellite P_{SAT}, showing that the pragmatic capacity using an increasing number of satellites improves.

V. CONCLUSION

The paper has examined the impact of phase uncertainty in the case of user-centric multi-satellite diversity. It has been shown that NCJT achieves unsatisfactory results especially in terms of system fairness among users when satellite diversity is adopted. However, a coarse synchronization of the transmitting devices restores a significant share of the gains achievable in the PCJT case.

REFERENCES

[1] M. Giordani and M. Zorzi, "Non-terrestrial networks in the 6G era: Challenges and opportunities," *IEEE Network*, vol. 35, no. 2, pp. 244–251, Apr. 2021.

[2] M. M. Azari, S. Solanki, S. Chatzinotas, O. Kodheli, H. Sallouha, A. Colpaert, J. F. Mendoza Montoya, S. Pollin, A. Haqiqatnejad, A. Mostaani, E. Lagunas, and B. Ottersten, "Evolution of non-terrestrial networks from 5G to 6G: A survey," *IEEE Commun. Surveys Tuts.*, vol. 24, no. 4, pp. 2633–2672, Aug. 2022.

[3] H. Xie, Y. Zhan, G. Zeng, and X. Pan, "LEO mega-constellations for 6G global coverage: Challenges and opportunities," *IEEE Access*, vol. 9, pp. 164 223–164 244, Dec. 2021.

[4] S. Buzzi, G. Caire, G. Colavolpe, C. D'Andrea, T. Foggi, A. Piemontese, and A. Ugolini, "Multi-satellite diversity through the use of OTFS," in *39th International Communications Satellite Systems Conference (ICSSC 2022)*, Oct. 2022.

[5] S. Buzzi, G. Caire, G. Colavolpe, C. D'Andrea, T. Foggi, A. Piemontese, and A. Ugolini, "LEO Satellite Diversity in 6G Non-Terrestrial Networks: OFDM vs. OTFS," *IEEE Communications Letters*, vol. 27, no. 11, pp. 3013–3017, Nov. 2023.

[6] S. Buzzi, C. D'Andrea, A. Zappone, and C. D'Elia, "User-centric 5G cellular networks: Resource allocation and comparison with the cell-free massive MIMO approach," *IEEE Transactions on Wireless Communications*, vol. 19, no. 2, pp. 1250–1264, Feb. 2020.

[7] Ö. T. Demir, E. Björnson, L. Sanguinetti *et al.*, "Foundations of user-centric cell-free massive MIMO," *Foundations and Trends® in Signal Processing*, vol. 14, no. 3-4, pp. 162–472, 2021.

[8] A. Guidotti, A. Vanelli-Coralli, and C. Amatetti, "Federated cell-free MIMO in non-terrestrial networks: Architectures and performance," *IEEE Transactions on Aerospace and Electronic Systems*, pp. 1–28, Feb. 2024.

[9] G. Bacci, R. De Gaudenzi, M. Luise, L. Sanguinetti, and E. Sebastiani, "Formation-of-arrays antenna technology for high-throughput mobile nonterrestrial networks," *IEEE Transactions on Aerospace and Electronic Systems*, vol. 59, no. 5, pp. 4919–4935, Oct. 2023.

[10] L. Gaudio, G. Colavolpe, and G. Caire, "OTFS vs. OFDM in the Presence of Sparsity: A Fair Comparison," *IEEE Transactions on Wireless Communications*, vol. 21, no. 6, pp. 4410–4423, Jun. 2022.

[11] 3GPP Technical Specification Group Radio Access Network, "Study on New Radio (NR) so support non-terrestrial networks," 3rd Generation Partnership Project (3GPP), Technical Specification (TS) 38.811, Sep. 2020.